Eindhoven University of Technology
Eindhoven, The Netherlands
April 21, 2024

Cross-section and shape optimization of three-dimensional plywood reciprocal frame structures based on raw material

M..J. de Munnik

*Department of the Built Environment, Structural Engineering and Design
Eindhoven University of Technology, The Netherlands
m.j.d.munnik@student.tue.nl

Abstract

To reduce environmental impact, structures should be made from environmentally friendly material and the waste of material during production should be minimized. Plywood reciprocal frames can potentially offer a solution that exploits the fact that relatively short members are used in reciprocal structures. This namely offers the opportunity for sustainable construction because it allows structural elements to be retrieved from standardized plywood products. Prior research on reciprocal structures has not adequately addressed the structural optimization of individual elements in reciprocal structures. Additionally, there has not been any focus on the minimization of waste material. In order to tackle those untapped areas of research, a reciprocal frame design tool has been developed that can generatively design a reciprocal structure based on a set of parameters and optimize the cross sections to be able to sustain Eurocode loading and fulfill Eurocode 5 unity checks.

The reciprocal frames are generatively designed by applying the center-to-center method (controlled by the *scale factor* parameter) on a two-dimensional tessellation. The tessellation mainly decides what the resulting structure looks like and is controlled by a set of parameters (*base size, pattern type, edge size and density gradient*). The resulting two-dimensional reciprocal frame is then inflated to a three-dimensional structure by moving the z-coordinates of the beam nodes. The correct geometry is found by mathematically minimizing the geometric 'error' by using the L-BFGS-B algorithm, that performs a directed search for the optimal solution. After the geometry is found, the individual sections are optimized using a custom by-part optimization process.

How the resulting geometry can be obtained as efficiently as possible from the (standard) plywood sheets is determined by (a) bin-packing algorithm(s). As a result, the number of sheets required to produce the structure is known. Therefore, the reciprocal frame designer can be seen as a black-box function with the design parameters as input and the number of sheets as output. This black-box function is used to optimize the initial set of design parameters. Firstly, an initial exploration has been performed to find the areas of interest. The resulting area of interest is often a tessellation edge size where two rows of beam elements can be obtained from one sheet. Within this area of interest, the set of parameters resulting in the least amount of plywood sheets is deemed the optimal reciprocal frame.

There are multiple layouts for each tessellation pattern that result in the lowest amount of plywood sheets. Generally, the smaller the scale factor, the more optimal the structure. The most optimal tessellation patterns are the triangle pattern and the square pattern. The other patterns are less efficient due to the inconsistent beam lengths or the relatively large beam lengths resulting from the tessellation geometry.

Keywords: Reciprocal frame, structural optimization, plywood, sheet material, parametric optimization, waste-material, innovative structural design, digital fabrication

1. Introduction

The building industry is becoming increasingly aware of its responsibility towards the environment. In the Netherlands, the built environment is responsible for 38% of the total CO_2 emissions [1]. A solution to become more environmentally sustainable is the use of climate friendly materials. Timber is an example of a climate friendly material, it can however only be considered climate friendly when it is harvested sustainably and used optimally. Therefore, it is important to focus on waste minimization when designing with timber.

When sawn timber is harvested from a tree (or log), around 50% of the log is considered to be waste material [2]. In contrast, for plywood only 25% of the log is considered to be waste material [3]. This is a direct result of the way plywood is produced; plywood is obtained by peeling a log and glueing several peeled layers.

Besides using climate friendly materials and minimizing waste material it is also important to motivate society to become more climate-conscious. A study by Kellert et al. [4] suggests that buildings with connections to nature, such as those constructed with natural materials like timber, can lead to improved health and well-being as well as more sustainable behaviour.

Combining the methods to become more environmentally sustainable has resulted in the research topic of plywood reciprocal structures. Reciprocal structures are structures where the (beam) members cooperate by supporting each other, and being supported by each other. This structural layout results in structures consisting of relatively short members with respect to its span. The fact that relatively short members are used offers an opportunity for the usage of plywood as base material.

Previous research on reciprocal structures has predominantly focused on design methods, design tools and the aesthetics of reciprocal fames. Some attention has been given to structural computation and checks according to international codes (e.g. Eurocode) [5], [6]. Additionally, some researchers have focused more on the geometrical optimization of reciprocal frames. For example, in a research by Y. Su et al. reciprocal structures were optimised by moving the nodes of the elements to minimize the strain energy of the structure [7].

Prior research has not adequately addressed the material optimization of reciprocal structures yet. Currently, there is no published research on the cross-section optimization or geometrical optimization of reciprocal structures. Additionally, the amount of raw material (e.g. number of plywood sheets) required to construct the reciprocal frame is not considered in any previous research on reciprocal frames. This represents an untapped area for improving the efficiency of reciprocal structures, resulting in the following research question:

*What approach can be used to **generatively design** and **digitally fabricate** an **optimized** three-dimensional reciprocal frame structure on a rectangular floor plan minimizing the amount of **standard plywood sheets** required?*

This research aims to show the opportunities of optimizing (reciprocal) structures based on raw material instead of structural volume by answering the research question. Additionally, the efficiency and opportunities of reciprocal structures are displayed.

2. Method

To answer the research question, a tool is developed that generatively designs a three dimensional reciprocal frame on a rectangular floor plan based solely on a number of parameters without any additional user intervention. During the generative design, the individual cross-sections of the reciprocal frame are optimized to satisfy Eurocode checks under certain loading conditions. The output of the generative design (and optimization) tool should be data that can be interpreted for digital manufacturing.

The resulting reciprocal frame designer can be considered a black-box function that returns a structural design based on the design parameters (see Figure 1). Using this black-box function, the design parameters are optimized using a multivariate Bayesian optimization. The optimization of the design parameters is focused on finding the combination of parameters that generates the structure that can be obtained from the smallest number of plywood sheets.

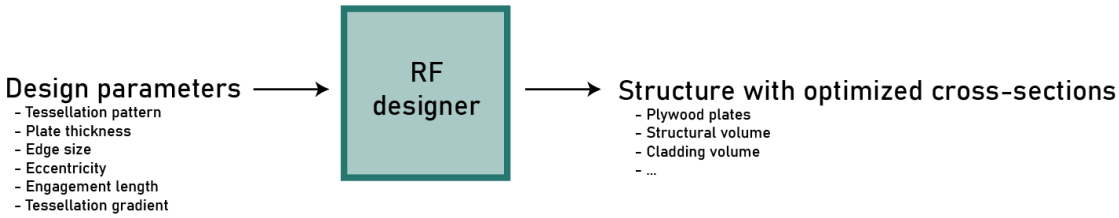

Figure 1: The reciprocal frame designer tool schematized as a black-box function

3. Literary review

3.1. Reciprocal frame design methods

Reciprocal frames are often designed based on a polygon tessellation. In literature, four analytical methods can be found for transforming a tessellation into a reciprocal frames: the translation method, the rotation method, the extended translation method and the center-to-center method [8], [9], [10]. These methods are applied to each polygon in a tessellation. The resulting line geometry is later connected using methods depending on the selected transformation method.

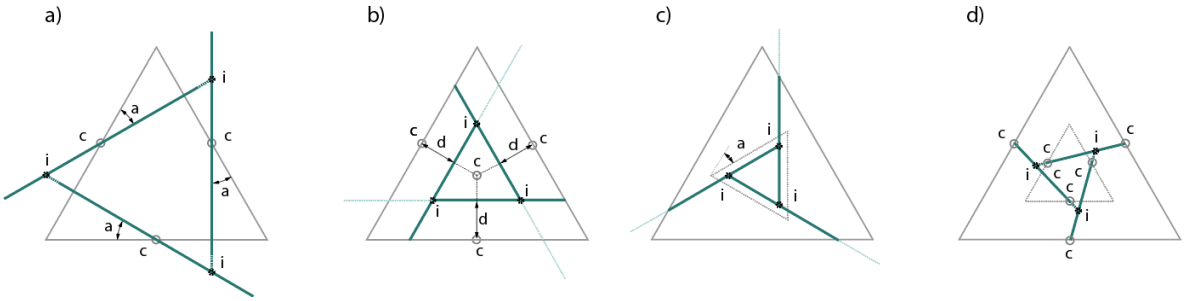

Figure 2: Reciprocal frame design methods for polygons. a) rotation method, b) translation method, c) rotation and translation method, d) center-to-center method

In this research, the center-to-center methods is applied. The center-to-center method naturally creates a regular grid when using basic polygons. The center-to-center methods is based on polygon scaling instead of transformations. Therefore, the resulting reciprocal frame is found by a single scaling factor, which determines the position of the intersection point of two joining elements. Additionally, intersections with neighbouring polygons are automatically created because all elements start on the center of the edge contrary to the other design methods.

In some inconsistent polygon layouts (e.g. a tessellation with a combination of squares and triangles) kinked members may be generated when combining the reciprocal units. These kinks are straightened by connecting the ends of the two beams and omitting the center node.

3.2. Form finding methods

Previously mentioned design methods are based on two dimensional tessellations and will thus result in two dimensional reciprocal frames. Transforming a two dimensional reciprocal structure into a three dimensional reciprocal structure requires additional form finding.

Due to the complex layout of three dimensional reciprocal frames, large reciprocal frames cannot be designed by free hand. In recent history, several methods to design three dimensional reciprocal frame structures have been developed. All of these methods are based on a starting with a design that roughly represents what the structure should look like, without complying to actual inter-member interaction requirements. This design then requires an iterative design process to generate a feasible design that does comply with all requirements to realistically simulate the interaction between the members.

3.2.1. 3D design methods

The first reciprocal frame structures were designed before iterative digital computation was available. Therefore, most early designs were made by trial and error [11]. In these cases, the interaction between the structural elements is not relevant as no additional (FE) calculations have to be performed.

A method to digitally transform a 2d reciprocal frame into a 3d structure is the mapping method, where a two-dimensional tessellation is mapped onto a three-dimensional surface. Mapping may result in a non-uniform reciprocal frame density. The mapping method will result in a structure that does not comply with the eccentricity requirements, therefore additional form finding methods need to be used to satisfy these conditions

Another method of transforming a 2d reciprocal frame to a 3d structure is by lifting the elements into a 3d shape [12]. This method is performed by moving each element until eccentricity requirements are roughly satisfied. Similarly to the mapping method, additional computation is required to satisfy all interaction conditions.

3.2.2. form finding techniques

With increasing computational speed of computers, iterative solver methods can be used to determine the exact geometry of reciprocal frame structures. Iterative solvers compute the best geometry solution of a reciprocal frame by selecting the best fitting value from a set of alternatives. The most optimal solution is found by minimizing an error function. For reciprocal structures, the problem is often defined by fining the ideal eccentricity between members:

$$\min f(error) = sum|e_{act} - e_{req}| \tag{1}$$

Several researchers have used this form finding method. Song et al. have used the method to keep the reciprocal frame as close as possible to the basic surface during the optimization procedure [13]. Su et al. have made a more advanced iterative solver, using bar elements, which allows finite element computations [14]. In this study, the error function was extended to a combination of the length condition, perpendicular condition and colinear condition. All of these researches have used a non-indeterministic algorithm. This means that the numerical method can perform a directed search to find the optimal structural shape.

Alternatively, dynamic relaxation is often used to find the correct geometry of 3d reciprocal frames. This method is fully deterministic, meaning that no randomness is involved in the form finding procedure. Dynamic relaxation uses fictional bending forces applied at undeformed regular grid structure forcing it to transform into a reciprocal frame, where balance is found by means of kinetic energy dissipation.

Dynamic relaxation also requires iterations to convert to a solution. The number of required iterations depend on the optimization procedure and the degrees of freedom in the structure. The complexity of dynamic relaxation can be expressed as: $O(n * m)$. Where is the number of degrees of freedom and m is the number of iterations required to find a solution. An advantage of dynamic relaxation is that it allows to use the same structural model for form finding and for structural analysis.

3.3. Digital manufacturing of plywood

The primary fabrication techniques for timber plate (2D) materials are CNC-routing, laser cutting, and waterjet cutting. Laser cutting, although commonly used, has limitations and is typically restricted to timber plates with a thickness of approximately 12mm. This limitation can be impractical for structural elements, making laser cutting less suitable for further consideration in this research.

Waterjet cutting, on the other hand, is a versatile cutting method that employs a high-pressure water jet to cut a wide range of materials. Despite being counterintuitive, waterjet cutting can be effectively used with plywood products [15]. This technique offers advantages over CNC-routing, such as the absence of heat influence during cutting and the ability to achieve highly precise contours. In general, regardless of plywood thickness, it is necessary to maintain a 3mm gap between elements to accommodate tabs that prevent parts from moving during cutting. The internal corner radius can be as small as 0.4mm

CNC, an acronym for Computer Numerical Control, employs a computer program to control machine tools. In the case of CNC-routing, a hand-held router serves as the spindle for cutting various materials. Unlike waterjet cutting, the plate thickness affects the thickness of the cutter and the minimum internal radius in CNC-routing applications.

The cutter thickness plays a significant role in determining the final cutting layout. The cutter thickness refers to the diameter or width of the cutting tool used in the CNC machine. , the company Plywood + Panel made table with general design parameters for cutting plywood plates with certain thicknesses (see Table 1**Error! Reference source not found.**).

Table 1:CNC guidelines acc. Plywood + Panel [16]

Thickness plywood (mm)	CNC Cutter Width (mm)	Min. Internal Radius (mm)	Minimum Gap (mm)
0-6mm	6	3	6
7-15mm	8	4	8
16-19mm	10	5	10
20-30mm	12	6	13**
> 30mm	16/20 mm*	8/10	17/21**

For thicker plates, the cutter width may depend on the hardness of the plywood (*), and the gap between cut elements is increased with 1mm to allow for a roughing pass (**). All CNC milling tools have a cylindrical shape and will create a radius when cutting an internal pocket. If internal edges with sharp corners are required (for example, when a part with rectangular shape needs to fit in the cavity), instead of reducing the radius of the internal edges, use a shape with undercuts.

Generally, CNC may be more restricting and complicated compared to waterjet cutting. However, CNC is widely applied in the Netherlands and should therefore be an available option for producing the reciprocal frame.

4. Design assumptions

Before being able to make the reciprocal frame design (and optimization) tool, some preliminary design choices must be made. The most important assumption to make is the element shape, as this influences the internal forces and the connection behaviour of the structure. An additional assumption that must be made is the cladding design is it influences the way the forces are applied to the reciprocal structure.

4.1. Element shape

The beam elements within a reciprocal structure serve as the fundamental load-bearing components that transfer the forces through the system. Optimizing their morphology involves refining their shape to maximize their capacity while minimizing material usage. Since the reciprocal frame structure is made of plywood, the structural elements must be planar elements.

Structurally, the beam elements have the function to support other beams along the span and be supported at the ends. The required support (end) conditions of the beam play an important role in the design of the members. The following conditions apply at both ends where the beam is supported:

- Lateral and vertical support: Displacement in both lateral directions and in the vertical direction must be prevented
- Torsional support: providing stability against rotation around the beam axis.

An additional requirement for sustainability is the minimization of non-sustainable connectors. Therefore layouts that use non-timber materials in the connections are filtered out. The support conditions and sustainability requirements result in four possible designs as visualized in Figure 3.

In design 1 and 2, the beams are supported by ‘consoles’ at the ends of the beams at the top of the beam. In design 1, tension forces are generated by clamping the ends to the adjacent beams. in the other design, dowels are used to clamp the beams between the adjacent beams. In design 3 and 4, the ‘consoles’ and holes are placed in the center. The difference between design 3 and 4 is the way how the eccentricity is created between the members. In design 3, the eccentricity is created by lowering the ‘consoles’ and in design 4, the eccentricity is created by raising the holes.

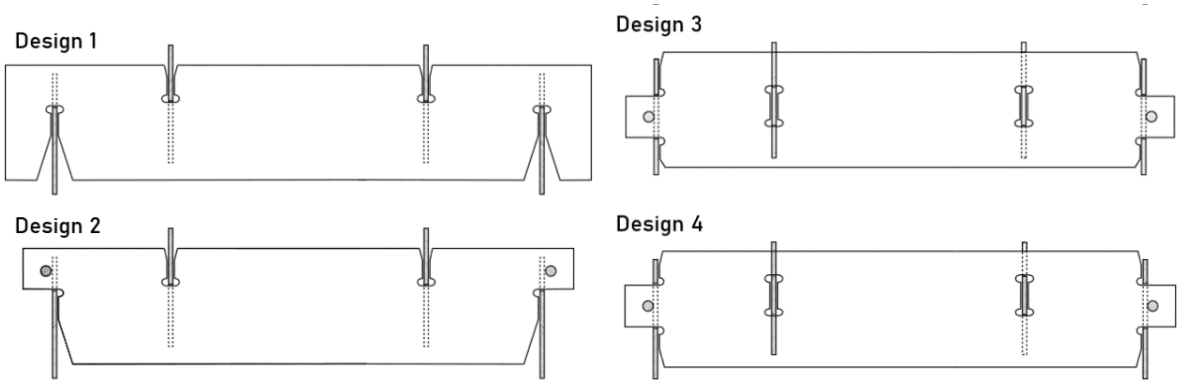

Figure 3: Beam morphology design options considered in the selection of most optimal beam shape in three-dimensional reciprocal frame structures from plywood sheets

The optimal design was selected based on a qualitative and quantitative comparison. In design 3, the holes that are used to support the adjacent beams are placed in the most favourable locations (where the bending stresses are the lowest). Additionally, the ‘consoles’ are placed lower, creating a lower shear stress concentration.

The beams are compared quantitatively by comparing the required dimensions in the ULS in three different locations in a reciprocal frame under Eurocode snow and wind loading (see Figure 4). The reciprocal frame that is used in this case is a 6x6m reciprocal frame with a central height of 3m and a squared pattern. The locations in the reciprocal frame that are used for the comparison are depicted in (with respective governing load case):

a) Extreme bending in M_{zz} direction (accumulated snow load)
b) Extreme bending in M_{yy} direction (distributed snow load)
c) Extreme compression N (distributed snow load)

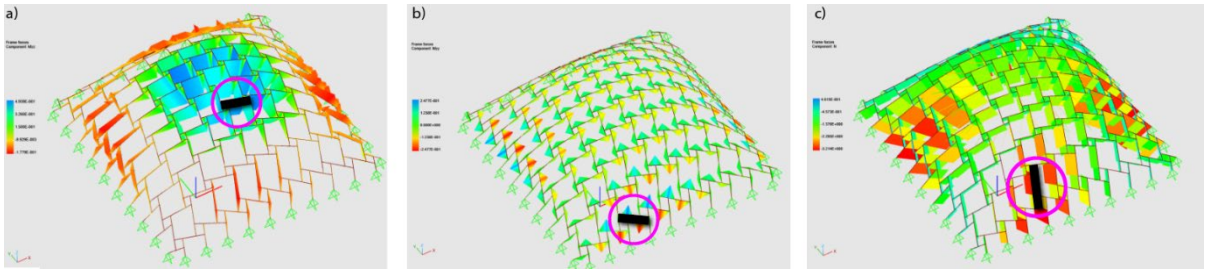

Figure 4: Beam locations for design comparison. a) Heavily loaded in M_{zz} (load displayed is accumulated snow load) b) Heavily loaded in M_{yy} (load displayed is distributed snow load) c) Heavily loaded in N (load displayed is distributed snow load)

The result of the comparison is summarized in Figure 5, where the optimal layouts are compared for different beam thicknesses. For each layout, the console heights, beam height, corner radii and gap heights are optimized to create the smallest overall section. Peterson's stress concentration factors were used for the determination of the stress concentrations [17]. In almost all cases, design 3 is the most optimal beam morphology. Therefore, design 3 is used for the remainder of this research.

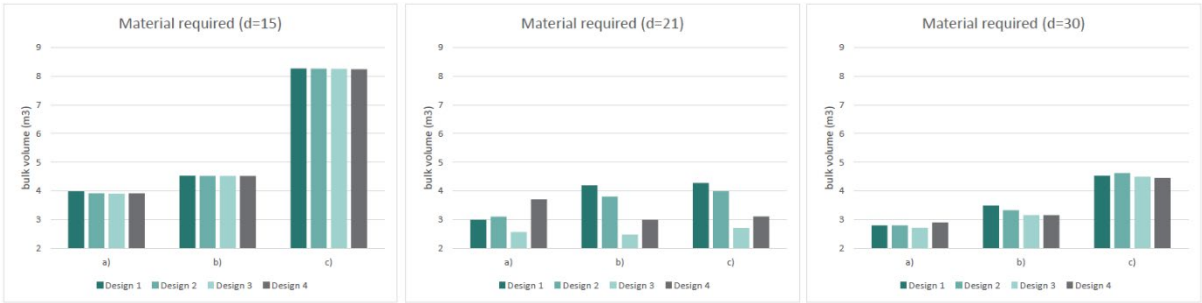

Figure 5: Bulk material volume required for each design variants for each of the locations. Left to right: plate thickness 10mm, 21mm and 30mm

4.2. Connection behaviour

A crucial element in accurately modeling reciprocal structures involves specifying the nature of the connection between the beam elements. The structure is stable when all connections are considered as pure hinges. However, the actual design of these connections may lead to a more rigid behavior. This rigidity may lead to a decrease in the bending moment midspan of the beams while introducing a bending moment in the connections. An important assumption in traditional structural analysis is that joints are treated as either perfectly rigid or perfectly hinged. Consequently, when assessing a structure, joints are typically simplified as being either fully fixed or fully hinged. In reality, structural connections rarely exhibit either perfect rigid or perfect hinge conditions [18].

To determine the actual connection behaviour, the connection stiffness will be evaluated through Finite Element Method (FEM) modeling in Ansys. Since the connection is entirely parametric, it is necessary to examine all potential connection configurations. This assessment will focus on the connection's response to bending in both of the primary directions.

Theoretical background

McGuire examined the issue of semi-rigid connections in dynamically loaded beams of an unspecified material [18]. He developed a continuum for joint stiffness versus normalized minimum natural frequency. To quantify the stiffness of a joint, he defined the joint stiffness a_{ij} as:

$$a_{ij} = \frac{kL}{E_b I_b}$$

where k = rotational stiffness of the connection, L = beam length, E_b = modulus of elasticity of the beam, and I_b = second moment of area of the beam. McGuire demonstrated that when $a_{ij} < 1$, pinned behaviour occurs because the deformed shape is similar to that of a pinned connection. He identified rigid behaviour when $a_{ij} > 100$, as the deformed shape closely resembles that of a beam with fixed ends.

The inter-member joints are designed as visualized in Figure 6, allowing for variations in the heights of the beams and the console. Furthermore, the dowel's size may vary. The joint stiffness for the entire range of design possibilities will be examined, considering the following design variables (with their respective variable ranges):

- Dowel size *5 – 20 mm*
- Beam height *88 – 400 mm*
- Beam thickness *10 – 50 mm*
- Eccentricity *0 – 50 mm*

A FEM model in Ansys is used to determine the actual joint behaviour. In the model, the plywood is modelled as a linear elastic orthotropic material. The linear elastic properties are determined from a research on plywood connections [19], and yield properties are determined from research on the in plane mechanical properties of plywood [20]. Within the FEM model, no post-yielding capacity is taken into account for the plywood. This means that the post-yielding tangent modulus is set to 0 MPa. The yield criterion used in the FEM model is the Hill yield criterion, which closely aligns with the actual yield behaviour but it may slightly overestimate the materials capacity [20].

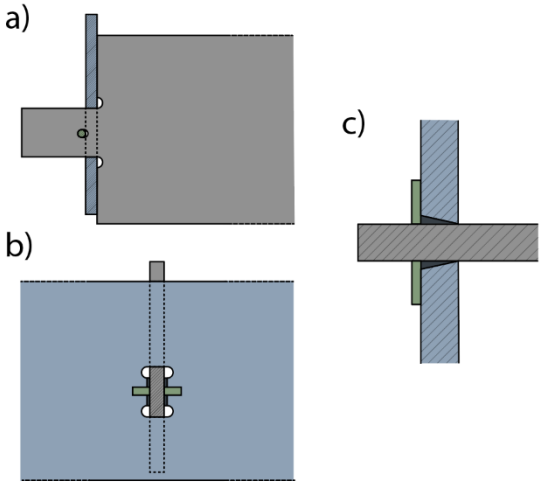

Figure 6: Connection details, where blue = beam 1, grey = beam 2 and green = dowel. a) side view, b) front view and c) top view

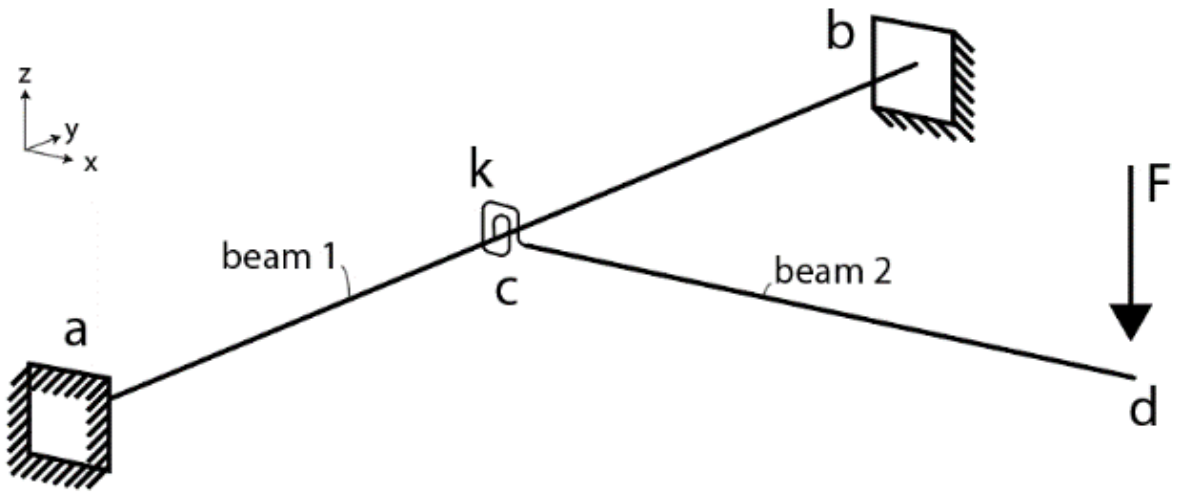

Figure 7: Structural scheme used to determine joint stiffness (for weak direction force F acts in positive y-direction)

To attain the pure joint stiffness behavior, it is necessary to establish the moment-rotation characteristics. This is achieved by employing the structural configuration depicted in Figure 7. The displacement in node d can be decomposed in the following components (when F acts in the -z direction): rotation of beam 1, bending of beam 2 and rotation in the joint c. In the case that F acts in the y direction, the displacement in d can be decomposed in: bending in beam 1, bending in beam 2 and the rotation in joint

c. To isolate the displacement attributed to the joint, the deformation of d in the case $k = \infty$ is subtracted from the total deformation.

The resulting joint stiffnesses in the weak bending direction of the beams are visualized for different parameters in Figure 8. For the joint stiffnesses in the strong bending direction, the results are visualized in Figure 9. In the figures, a_{ij} is shown for beams with a length of one meter.

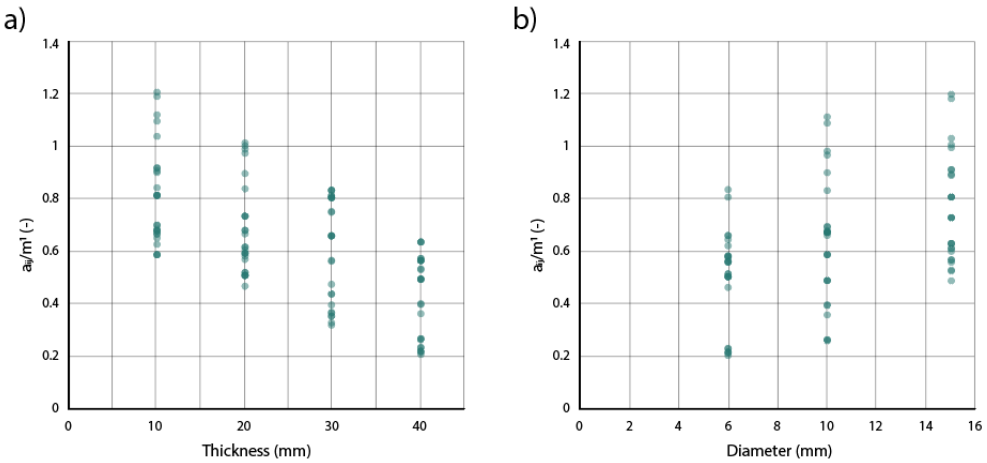

Figure 8: a_{ij}/m^1 in the weak bending direction, for a) different plate thicknesses, b) Different dowel diameters. Derived from Ansys models.

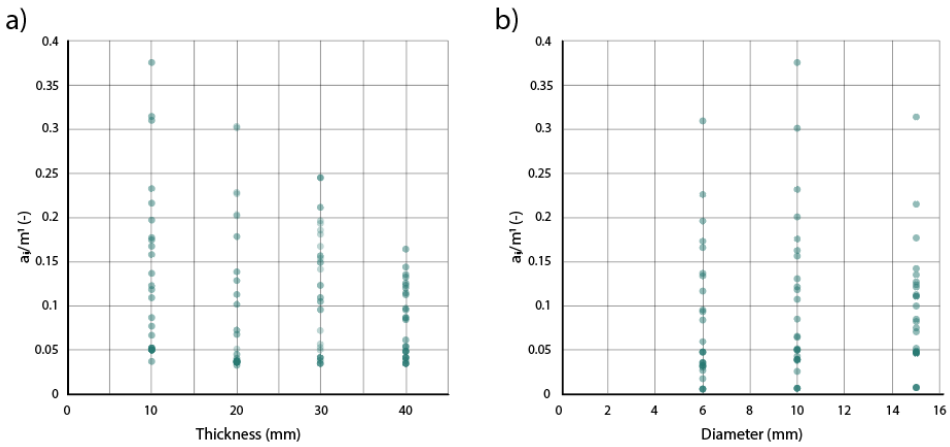

Figure 9: a_{ij}/m^1 in the strong bending direction for a) different plate thicknesses, b) different dowel diameters

In both bending directions, one could say it is reasonable to assume hinged behaviour between the elements, since the values are almost always below 1.0. An additional risk analysis has been performed to ensure that assuming hinged connections does not result in structural failure. In the risk analysis, the internal forces are compared for the same structure with all connections being hinged or all connections being rotationally fixed. Multiple squared-based reciprocal frames are considered, with different sizes (between 8x8m and 2x2m) and eccentricities (and thus curvature). In these calculations, the scale factor is 0.5 and the density gradient is 0.

From the risk analysis, it was concluded that for the weak bending direction, the bending moments in the middle of the beams may be underestimated in some cases (by a maximum of 10%). This underestimation is considered to be within the limits of safe design, especially because the connection is not close to being purely fixed.

In the strong direction, assuming hinged connections is relatively safe. The only problems may occur at the ends of the beams where the moment is underestimated if the connection would be fixed. To make a conservative assumption in the connection calculations, 5% of the bending moment in the middle of the beam are added to the bending moments at the ends to prevent failure due bending at the beam ends.

4.3. Cladding

The assumed cladding concept for the optimization in this research is based on the cladding that was applied in the 'Dome of Visions' [21]. Each connection between the beam elements of the reciprocal frame is also a nodal connection to the cladding. This connection is applied at the ends of the beam elements. Figure 10 shows the detail of how the cladding is connected to the beam elements as well as how the layers of polycarbonate are connected. The holes in the polycarbonate sheets are oversized, making sure that no normal forces can be transferred along the plane of the cladding.

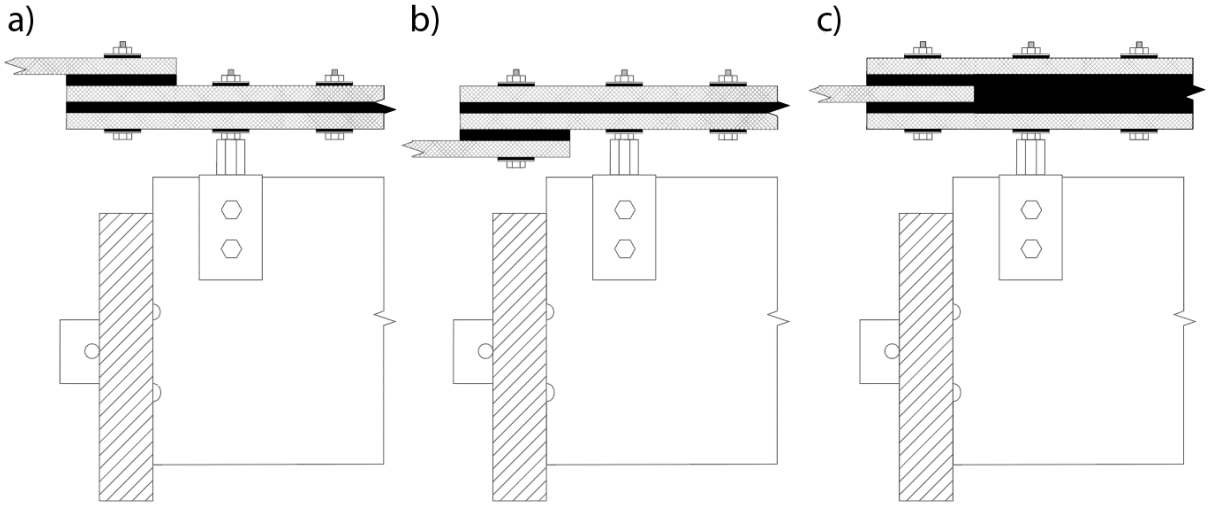

Figure 10: Cladding connection and layer detail at three different locations

The connection to the cladding is designed in a way that the cladding does not transfer normal forces along the plane. Therefore, bending moments must be transferred through the connection. The amount of bending moment that is transferred through the connection depends on the angle at which the force is applied with respect to the connector. The horizontal component of the force is used to calculate the moment that is applied at the node: $M_{ecc} = F_{hor} * a$. The arm a is half of the beam height + 20mm that is used as a standard distance from the beams.

5. Reciprocal frame designer

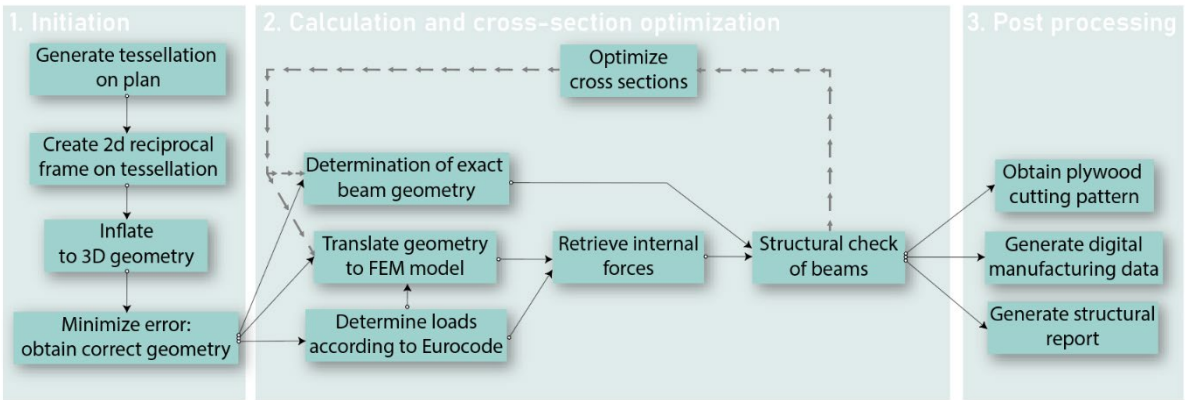

Figure 11: Flowchart of the reciprocal frame designer

The workflow for the generative reciprocal frame designer is described using the flowchart in Figure 11. The workflow consists of three main phases:

1. Initiation: creation of a reciprocal frame geometry based on several design parameters.
2. Calculation and cross-section optimization: obtaining data required for calculating unity checks of the beam elements and performing these unity checks.
3. Post processing: turning the checked and optimized reciprocal frame into usable data for digital manufacturing and a calculation report.

5.1. Tessellation

The reciprocal frame designer generates a reciprocal frame on a two dimensional tessellation using the center-to-center method. The tessellations are laid over the user provided input rectangular plan. The tessellations applied in this research are equilateral polygon tessellation because all edges in such tessellations share the same location and there are no gaps in the tessellation. As a result, the middle points of each of the sides of the polygons are the same as for a neighbouring polygon, which is useful for the center-to-center method.

The equilateral polygon *tessellation patterns* that are considered in this research are visualized in Figure 12. Since the polygons are equilateral (i.e. have equal edge lengths) the whole tessellation can be scaled with a single factor*: tessellation edge size*. In the patterns in Figure 12, the original base 'plan' is displayed underneath the tessellation. As visible in the figure, the tessellation does not always exactly match the original floor plan. To obtain the tessellation with a certain edge size that matches the base plan as closely as possible, any polygons that do not have an edge in the plan are removed from the tessellation.

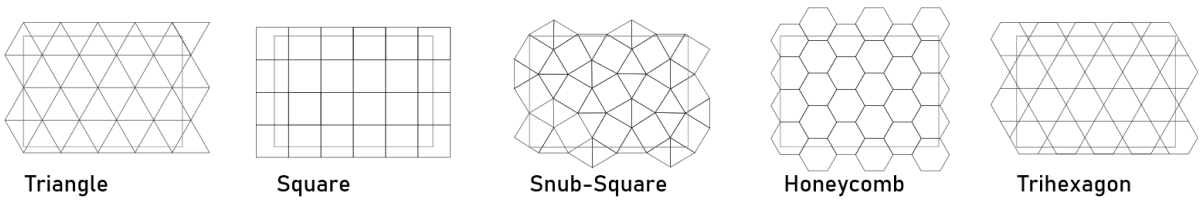

Figure 12: Tessellation pattern layouts considered in this research

Tessellation density gradient

By default, as a result of the equilaterality of the tessellation, the density of the tessellation is equal over the whole plane. For structural optimization and/or aesthetic reasons it might however also be interesting to increase or decrease the structural density in the middle of the structure or towards the edges. To achieve a higher density towards the center or edges of the reciprocal frame, the base 2d tessellation needs to have a variable density. The density behaviour is determined by the *gradient factor*. To gradually increase the density towards the center of the structure, the points are translated towards to center by a variable distance. This distance is determined by the following formula:

$$d = G_f(x) \times d_{center}$$

Where:

- $G_f(x) =$ value of the gradient function at point location x
- $d_{center} =$ distance of point to the center

The gradient function $G_f(x)$ is a parabola that is zero at min_x and max_x and has an extreme at the center. The value of the extreme is the gradient factor G that determines the degree to which the gradient is increased or decreased towards the center of the reciprocal frame. The natural boundaries of the gradient factor are [-1, 1], where -1 means all points have moved to the edges and 1 means all points have moved to the center. To create feasible reciprocal structure, in this research, the limits of G are [-0.3, 0.3].

5.2. 2d reciprocal frame

To turn the 2d tessellation into a 2d reciprocal frame, the center-to-center method as described in the literary review is used. The center-to-center method is applied by scaling each polygon in the 2d tessellation by *scale factor* S_v.

The single unit reciprocal frames must be connected to each other, to create a full reciprocal frame. The connection of these separate reciprocal frames is performed in the following steps:

1. Remove duplicate nodes
2. Merging beams that share a begin/end node
3. Recalculating the position of intermediate nodes

The first step, the removal of duplicate nodes, is simple; when a node shares the same x, y and z location, the node is removed. The second step, merging beams that share a begin/end node is a bit more complex. Figure 13 shows a graphical representation of how this is done. Firstly one of the beam elements is removed and the other beam element inherits the begin/end node ID from the removed beam. Secondly, the Begin/End support ID's are updated.

As visible in Figure 13b, the positions of the connecting elements are not always correct after the second step. This is fixed in the third step where the intermediate nodes are moved to the locations where the beam vectors intersect.

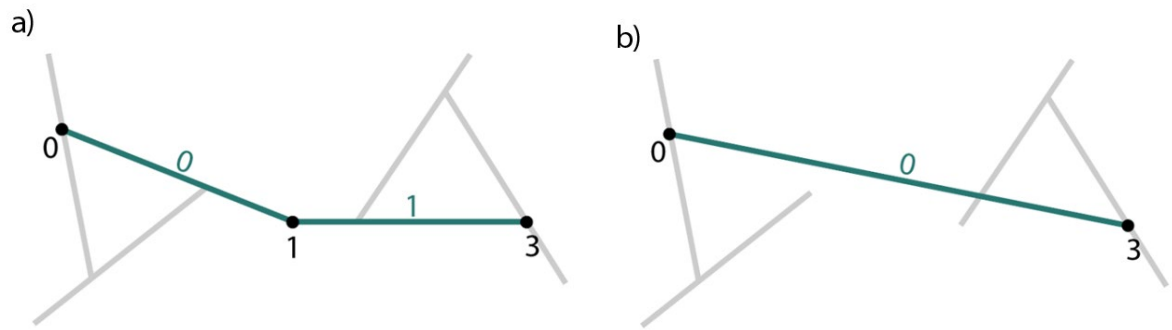

Figure 13: Step 2 of connecting the single unit reciprocal frames. a) initial condition, b) situation when the beams are connected

5.3. Inflation to 3d reciprocal frame

The 2d reciprocal frame is inflated to transform the 2d geometry into a 3d reciprocal frame structure. This inflation is achieved by creating an inter-member eccentricity. Directly determining the exact positions of each nodes for a frame with a specific eccentricity is mathematically impossible. There are however indirect solutions to solve this problem as mentioned in the literary review. In this research, a mathematical minimization is used to find the exact solution. To aid this mathematical minimization, it is important to estimate the position of the nodes as accurately as possible. This is done by inflating the structure by moving the z-coordinates of the nodes until convergence requirements are met.

With the introduction of inter-member eccentricity, also so-called connection beams are introduced. This connection beam is also used to check if the convergence requirements for the inflation are met. The connection beams are created by finding the point on the support beam that is the closest to the begin/end node of the beam.

When the connection beams are defined, the inflation can be performed by looping over all connection beams. The z-coordinate of the begin/end node of the main beam are increased by the required *eccentricity* for each connection beam that does not meet the initial connection beam requirements:

- $L_{connection\ beam} \geq e_{req}$
- $z_{N_{beam}} - z_{N_{connection}} \geq e_{req}$

In words: the length of the connection beam is equal to or larger than the required *eccentricity* and the z-coordinate of the beam node is *eccentricity* larger than the z-coordinate of the connection beam node. As a result, the *eccentricity* is the parameter that controls the amount of curvature there is in the reciprocal frame.

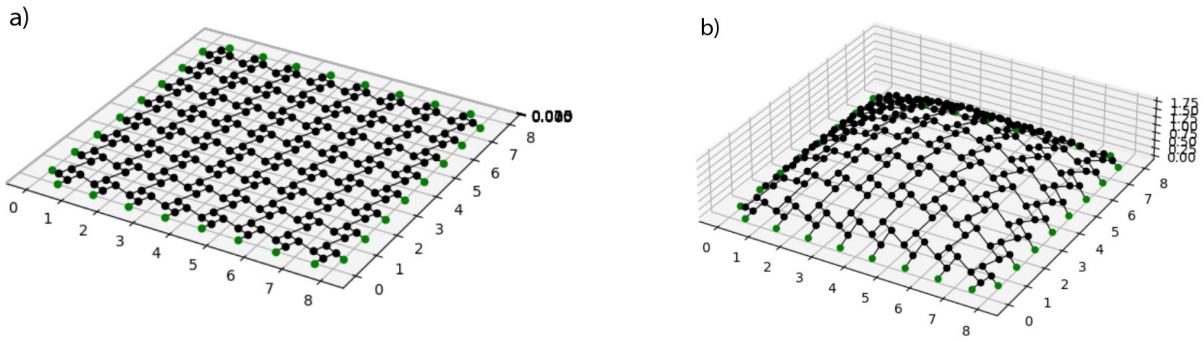

Figure 14: Reciprocal frame a) before and b) after inflation loop

Figure 14 shows the effect of the inflation on a typical reciprocal frame structure. The resulting 3d frame gives a good estimation that can be used for the mathematical minimization.

5.4. Minimizing model error

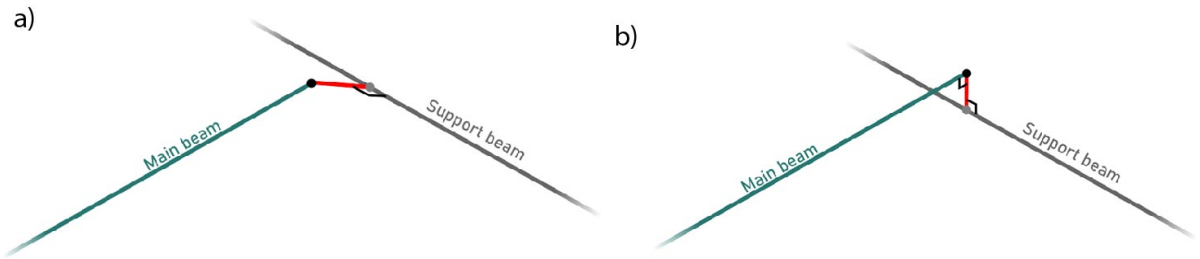

Figure 15: a) connection behaviour after inflation and b) correct connection behaviour

As mentioned before, the estimated 3d reciprocal frame does not represent the actual structural behaviour of the structure. Figure 15a indicates the structural shape that may be found after inflation. When there is an eccentricity between elements, the eccentricity member should always be perpendicular to both beams to correctly represent the structural behaviour. To make sure that both these conditions are met a mathematical minimization is applied that minimizes the model 'error'.

The error of each connection beam is calculated geometrically using the following formula:

$$E_k = |sin(\theta - 90) \times L_{cb}| + |\big(e - (\cos(\theta - 90) \times L_{cb})\big)|$$

Where:

- θ = angle between the main beam and the connection beam
- L_{cb} = length of the connection beam
- e = required eccentricity

The first part of the error function is the perpendicular condition. Since the connection beam is connected to the point on the support beam that is the closest to the end point of the main beam, the connection beam is always perpendicular to the support beam. This means that the perpendicular condition only looks at the angle between the main beam and the connection beam. The second term of the error is the length condition, where it is checked whether the length of the connection beam is equal to the required

eccentricity. The length condition is corrected for the perpendicular condition, which means that the error is larger when the angle is incorrect.

The error of the full model can be determined by combining the errors of each of the connections. The error of the full model is defined by the formula:

$$E = \sum_{k=1}^{n} E_k^2$$

In words this means that the error is the sum of the squared value of connection beams. The error values are squared to aid convergence when minimizing the model error.

Optimization problem

To find the values for each of the coordinates that results in a model error E that is (close to) zero, a mathematical optimization must be performed. The optimization problem is described as:

Minimize $E(x_n, y_n, z_n)$

Subject to: $x_n \epsilon\, \Omega_n$
$y_n \epsilon\, \Omega_n$
$z_n \epsilon\, \Omega_n$

This means that the model error, based on the node coordinates, must be minimized. The minimization is subject to constraints of the coordinates where each of the nodes are subject to a bounding box. To make sure that the 'optimized' solution maintains the shape and uniformity of the inflated geometry, the bounding box for each node is relatively small in x and y direction: bounding box = [(-2e, 2e), (-2e, 2e), (-1, 1)]

To solve the minimization problem, the L-BFGS-B optimization is used. The L-BGFS-B is a multivariate minimization algorithm. This algorithm is used because it is efficient in memory usage which makes it efficient for high dimensional problems. The L-BFGS-B algorithm finds a global minimum of the function by iteratively estimating a Hessian matrix. The Hessian matrix gives information about the curvature for all n dimensions of the problems. In other words; it tells which direction a variable should move to improve the global solution. This means that the L-BFGS-B algorithm performs directed searching to minimize the function result. This leads to relatively fast convergence for large scale problems.

6. Structural optimization

With the geometry of the three dimensional reciprocal frame known, the individual cross-sections can be structurally checked and optimized. The exact beam geometry must be determined before being able to calculate the internal forces and thus the dimensioning of the structural elements. The geometry must be determined based on limited information; the begin and end node location of the beams and the rotation of the section with respect to the base plane (which is determined by the connection lines).

The rotations at the beam ends are determined by casting the beam elements as planes. The vector that is the intersection between the planes can be computing the cross product of the two planes. The angle between the intersection vector and the beam vector gives the end rotation in the beam.

The planes are cast in two directions to determine the 3 dimensional end rotation, see Figure 16. In a), the planes are cast in the local x-z planes. The intersection vector (visualized in red) is the vector parallel to the intersection line, determining rotation θ_1. In b) the planes are cast in both the local x-y plane and x-z planes. The intersection vector determines rotation θ_2.

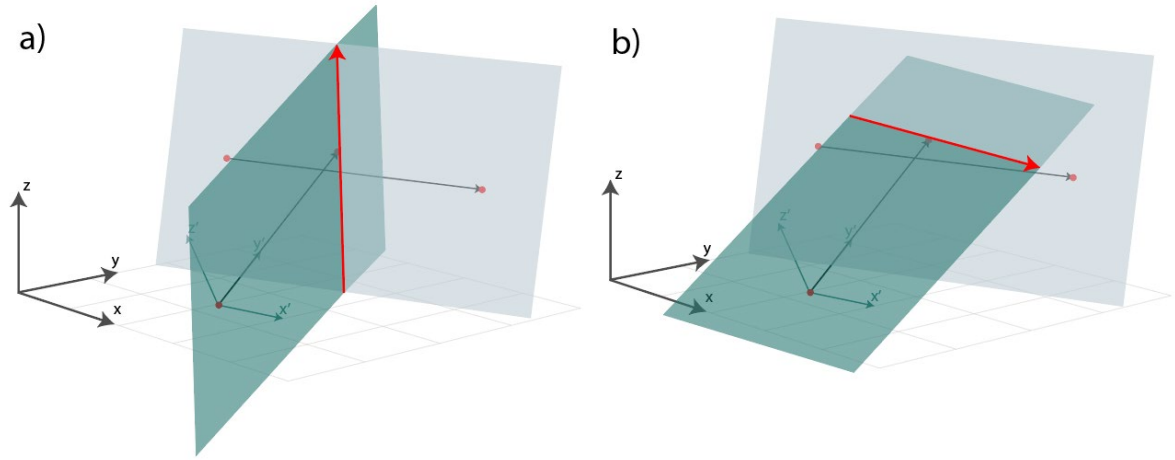

Figure 16: Beam elements cast as planes to determine end rotations

When the rotations at both the begin and the end of the beam are known, the rotations of the holes can also be determined. To fully determine the hole rotations, three angles need to be known. The first two can be determined by the end rotation of the adjacent beam$\varphi_1 = \theta_1, \varphi_2 = \theta_2$. The other rotation that must be known is the rotation around the central axis of the hole. This angle is determined by the rotation around the axis of the adjacent beam and the pitch of the hole beam:

$$\varphi_3 = \theta_{ax,adj} - \theta_{pitch}$$

6.1. FEM modelling

The reciprocal frame geometry must be transferred a finite element model to be able to calculate the internal forces in the structure. The internal forces are calculated by using a line model instead of a model with the exact geometry to be able to calculate the internal forces rather quickly. In the FEM line model, the beam elements are split up at the location of the connection line to create an intermediate node on the beam elements. Figure 17 shows how the beam elements are split into multiple FEM beam elements.

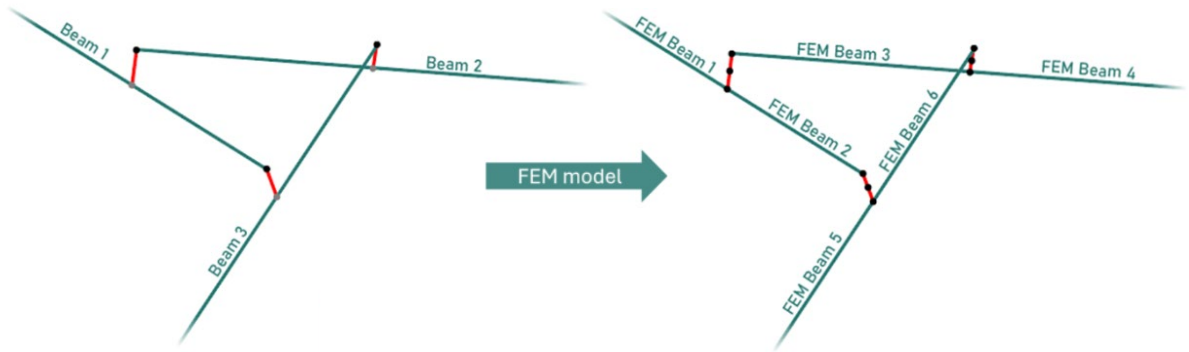

Figure 17: Reciprocal frame geometry translated to FEM model geometry

The inter-member connection behaviour in the reciprocal frame are determined previously as; hinged in M_y and M_z and fixed in M_x (rotation around the beam axis). This behaviour is achieved by creating an additional intermediate node on the connection beam. The intermediate node has the same rotational freedom as the full connection. The connection beam elements are modelled as being infinitely stiff, this means that the connection behaviour can be seen as either fully fixed or hinged (depending on the rotation direction). The nodes at the ends of the beams, and the intermediate nodes on the beam are considered to be fully fixed.

Table 2: Material properties plywood in the FEM model. Derived from[22].

Density	ρ	460	kg/m^3
Young's modulus	E_1	6682	MPa
	E_2	5318	MPa
	E_3	5318	MPa
Shear modulus	G_{12}	350	MPa
	G_{13}	52	MPa
	G_{23}	38	MPa
Poisson ratio	v_{12}	0.04	
	v_{13}	0.191	
	v_{23}	0.248	

In the FEM model, the plywood is assumed to behave linear-elastic orthotropic. Assuming linear-elastic behavior is safe when the stresses are expected to be rather low, which is the case when designing for stresses below yielding. The following material properties are assumed (see Table 2). These properties are expected to resemble plywood behaviour for various standard thicknesses. When the exact stiffness properties for a certain type of plywood sheet is known, they can manually be entered in the reciprocal frame designer tool.

The loads that are applied to the FEM model are determined by the Eurocode standard. In this research, the reciprocal frame will be loaded by (combinations of) permanent loads, imposed loads, wind loads, snow loads and temperature loads. For the wind loads, the structure is considered to be a flat roof (when the height is lower than 5% of the width), or a dome structure. In the reciprocal frame designer tool, the user can enter the (Dutch) wind area for where the structure is placed, this influences the amount of loading that takes place. For snow the load shapes for cylindrical roofs are applied as well as an equal distribution of snow load.

6.2. Stress concentration checks

The reciprocal frame designer performs all required Eurocode unity checks on the beams to ensure that no structural failure will occur. That includes stress checks, stability checks and connection checks. Additionally, due to the fact that there are holes in the beams, the stress concentrations around the holes will be checked.

In principle, two types of stress concentrations will occur in the beam elements:

1. Normal stress concentrations: caused by a combination of axial forces, bending in-plane of the element and bending out-of-plane.
2. Shear stress concentrations: caused by a combination of shear in the strong direction, shear in the weak direction and torsion.

These stress concentrations can be determined using FEM calculations. However, the beam calculations are part of an iterative process (cross-section optimization). Therefore, FEM calculations for each separate beam element would require excessive computation time. Too speed up the process of determining the stress concentration, a predictive model is made using 1.124 pre-calculated Ansys FEM calculations per load situation.

The pre-calculated Ansys FEM calculations aim to discover the full design range of the holes in the beams (variable, range):

- Ratio h/H : [0.1,0.9]
- Ratio r/H : [0.05,0.3]
- Ratio h/b : [0.1,0.5]
- $\theta_1, \theta_2, \theta_3$: [0°, 45°]

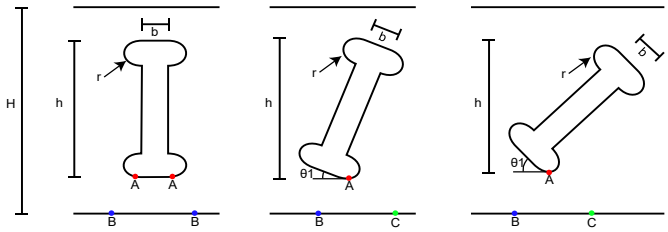

Figure 18: Variables used to determine the stress concentrations around the holes

Figure 18 visualizes the variables and the locations of the stress concentrations (A). $[\theta_1, \theta_2, \theta_3]$ is the three-dimensional hole rotation. Using the multiple pre-calculated Ansys simulations, a predictive model can be trained that predicts the stress concentration value K_t based on the known data. To make sure the predictive model is accurate, the model is trained with 80% of the data and tested with 20% of the remaining data.

Since linear elasticity of the material may be assumed according to the Eurocode, the stress concentration factors for each of internal force components may be calculated separately and superimposed to find the actual stress peaks.

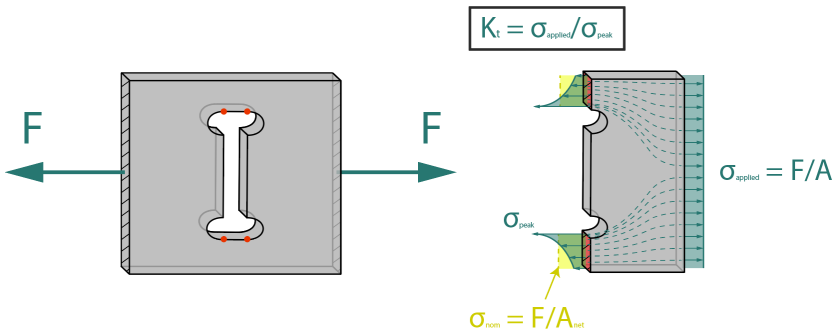

Figure 19: Graphical representation of stress concentrations due tension of the beam elements in the reciprocal frame.

As an example, the results for stress concentrations due to tension forces will be discussed. The location of the stress concentrations as well as the stress flow are visualized in Figure 19. In this case, the applied tension stress is simply calculated using $\sigma_{applied} = F/A$. The stress concentration value is calculated as $K_t = \sigma_{applied}/\sigma_{peak}$ where σ_{peak} is found by the FEM model.

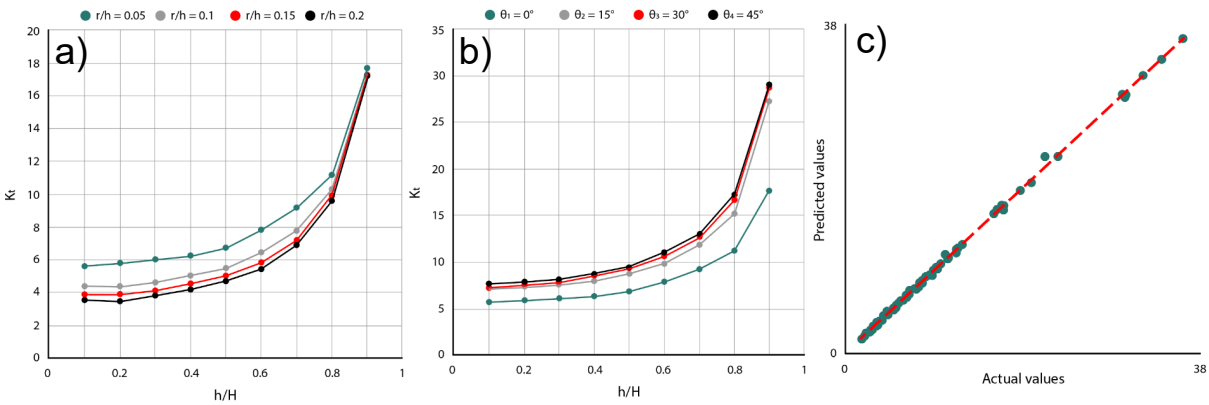

Figure 20: a) Stress concentration K_t around hole in pure tension, with h/b = 0.1 and θ = [0,0,0] for different values of r/h, b) Stress concentration K_t around hole in pure tension, with h/b = 0.1, r/h = 0.1 and $\theta = [\theta_1,0,0]$ for different values of θ_1 and c) Predicted vs. actual K_t values for stress concentration due to pure tension, with ideal line (red)

The resulting stress concentrations for h/b = 0.1 and θ = [0,0,0] are plotted in Figure 20a. As visible in the figure, increasing the hole height significantly increases the stress concentration around the hole. Additionally, the influence of the fillet radius can be seen from the plot. Increasing the fillet radius can quite significantly decrease the K_t value, especially when the h/H ratio is relatively low. Figure 20b shows the resulting stress concentrations for different rotations around the main hole axis (with h/b = 0.1, r/h = 0.1 and $\theta = [\theta_1,0,0]$). Here it can be seen that rotating the hole also has a significant influence on the stress concentration, as more rotation results in higher stress concentrations

Since all of the parameters influence the final value for the K_t value, a 6th order linear model is used to predict the value of K_t. Figure 20 shows the accuracy of the predictive model, as the predicted values are almost equal to the actual (training) data. The red line indicates where the points should be for perfect predictions. This means that the predictive model can quite accurately predict the K_t values. The accuracy of the fit is: $R^2 = 0.98$.

6.3. Section optimization

With all the unity check calculations in place, the cross sections can be optimized by finding the smallest possible beam dimensions that result in fulfilling all the unity checks. This optimization is performed by looping over the second phase of the reciprocal frame designer (see Figure 11). For the optimization of the beam dimensions, the following parameters can be optimized:

- Beam height: h_{beam}
- Console heights: tenon heights: $h_{ten,l}$ and $h_{ten,r}$
- Dowel radii: $r_{dowel,l}$ and $r_{dowel,r}$
- Fillet radius: r_{fillet}

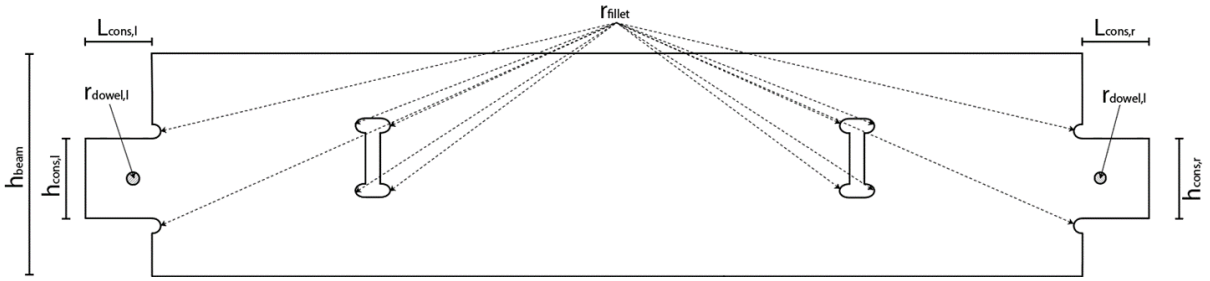

Figure 21: Beam with parameters that can be optimized in cross-section optimization

In practice, the fillet radius does not influence the stress concentrations significantly (because the ratio h/H is often quite low). Therefore, the fillet radius is not included in the optimization process. This results in a total of 5 parameters to be optimized for each beam element.

Optimizing each of the parameters using a mathematical minimization solver is not possible because the parameters of one beam directly influences the behaviour of adjacent beams. Additionally, mathematical minimization solvers can generate combinations of parameters that are not feasible. To overcome these problems in the section optimization, a custom part-by-part optimization technique is developed. The optimization technique consist of three main phases and an initiation phase.

Initiation

Since reciprocal frames are statically indeterminate, the internal forces are influenced by the cross sections of the structural elements. Initially, some geometry must be assumed to calculate the internal forces in the structure. In the cross section optimization process, the minimum possible beam heights are used to initially calculate the internal forces.

The unity checks of all structural elements are calculated using the initial internal forces. When all unity checks are satisfied, the minimum beam height is accepted as optimal solution. If this is not the case, the three phase optimization process is initiated.

Phase 1: tenon optimization

In phase 1, the minimum required heights for the tenons are calculated. These minimum tenon heights are based on the support stresses in the tenons and the shear in the tenons. The unity checks are performed for both tenons on each beam. When the unity checks are not satisfied, the tenon height is incremented with 1mm. Additionally, the beam height is incremented with 1mm to make sure the tenon is not larger than the beam height. When the unity checks are satisfied, the tenon height is accepted as minimum tenon height.

Phase 2: dowel optimization

The tension force in the tenon/dowel is dependent on the height of the beam since the beam height influences the arm between the dowel and the compression area. This means that in principle, for all dowel sizes, the unity checks can be satisfied.

To tackle this problem, the dowel dimension is sought which results in the lowest accompanying beam height. This is done by iterating over the possible dowel dimensions and storing their required beam height in a list.

For each beam, for both tenons, the list of dowels is iterated. The tenon height is the maximum height of either the tenon height found in phase 1, or the tenon height based on the edge distance requirements. For this combination of tenon and dowel, the beam height is computed so that the dowel unity checks are satisfied. When this is done for all of the possible tenon dimensions, the dowel dimensions resulting in the lowest beam height are accepted as optimal solution. Additionally, the beam height of the adjacent beam is incremented (if necessary).

Phase 3: main section optimization

When both the dowel and tenon dimensions are known, the unity checks of the main section and stress concentrations can be performed. To satisfy these unity checks, only the beam heights can be increased.

For all beams the unity checks for the main section and the stress concentration are performed. When the unity checks are not satisfied, the cross section height is increased with increment factor b. This process is looped until the unity checks are satisfied.

Convergence

The three main steps are looped until the unity checks are satisfied after computing the internal forces. In that case, the cross sections satisfy the unity checks with the actual internal forces corresponding to the structure with the same cross sections.

Mathematically, the convergence criterion can be described with the following formula:

$$\forall_i \; UC_i - UC_{max} \leq 0$$

This means that for all i's, the unity check minus the maximum allowed unity check value should be smaller than or equal to zero.

This cross-section optimization method can be seen as a *monotonic sizing optimization*. The optimization process is monotonic because the cross-section values can only be increased. This leads to fast convergence, but the found solution may not be the global minimum.

An additional constraint for the cross section optimization, besides element unity checks, is the global unity check of the maximum serviceability deformation. When the deformation is too large, all cross section heights are increased until the deformation requirements are satisfied. The deformation in practice was never found to be normative.

6.4. Bin-packing

After knowing the dimensions of the beam elements, it must be determined how much raw material is required to obtain the beam elements. To do so, bin packing algorithms are used to determine the most optimal way to place the elements in the sheet. Bin packing algorithms are so called NP-hard algorithms, which means there is no known algorithm that can solve all instances of the problem [23]. In the case of packing the beam elements in the plywood sheets, it means that there is not one algorithm that will give the most optimal result (global minimum). To tackle the NP-hardness, multiple bin packing algorithms are ran for each instance of the reciprocal frame; the shelf algorithm, guillotine algorithm, maximal rectangle algorithm and skyline algorithm [24]. Since the bin packing problems is an offline bin packing problem (all geometry is known before performing the algorithm), the beams can be sorted based on height or length) before bin packing [25]. This will typically aid the bin packing algorithm and thus result in fewer sheets required.

7. Parametric optimization

The optimization of structures is often based on minimizing the volume of the structural elements. A factor that is often forgotten in this optimization goal is the amount of material that is required to produce said structural elements. For plywood, a structure with optimized cross sections and a layout that results in the lowest beam volume may result in large amounts of waste material when the elements are obtained from the plywood sheets.

The geometry of the reciprocal fame is based on a set of design parameters: base rectangle dimensions, tessellation pattern, tessellation edge size, tessellation density gradient, scale factor and eccentricity. The sizes of the beam elements are in turn based on the load conditions, sheet thickness and maximum allowed value for the unity check.

For the optimization, the target is to find the combination of design parameters resulting in the most material-efficient reciprocal frame for certain span dimensions, when exposed to the user entered load conditions. The optimization problem can thus be expressed as:

Minimize $V_{sheets} = f(\mathrm{TP}, \mathrm{ES}, \mathrm{E}, \mathrm{SF}, \mathrm{DG}, \mathrm{T})$

Subject to:

- Plywood sheet size
- Maximum unity check
- Load conditions

The reciprocal frame designer is used to obtain the total volume of plywood sheets that is required for a certain combination of parameters. This can be seen as a black-box function; this means that the only thing known about the function is the value that comes out. For optimization algorithms this means that no additional information can be obtained from the function (e.g. the derivative function).

A second important consideration is the fact that evaluations are ‘expensive’ (i.e. time consuming). For large problems, the reciprocal frame designer may need several minutes to compute an optimized structure.

The Bayesian optimization algorithm suits the design space and problem best because the algorithm can make most out of limited evaluations. The algorithm is best-suited for optimization over continuous domains of less than 20 dimensions, and tolerates stochastic noise in function evaluations [26]. This means that the algorithm allows a non-smooth function, which is expected for the reciprocal frame results (a slight change in a parameter may result in more plywood sheets to be used and thus a jump in raw material volume).

The Bayesian optimization algorithm can be used to both explore and exploit the objective function. Exploration means that the algorithm is used to ‘explain’ the objective function without looking for an

optimal value. Exploitation means that the Bayesian optimization algorithm is used to search for the optimal value. When the Bayesian optimization algorithm focusses too much on exploitation, a global minimum value may be missed.

In this research - for the design space of optimizing the reciprocal frame dimensions - the most effective acquisition function is the expected improvement function. The reason for this is that it is focused on finding a global minimum. Additionally, the expected improvement function has the quality of handling a noisy objective function. The amount of exploration/exploitation when using expected improvement can be tuned with the parameter x_i which is between 0.0 (prefer exploitation) and 0.1 (prefer exploration). In this research, the x_i parameter is set to 0.01. This means that the optimization is focused on exploitation, to be able to quickly find optimum results.

Before applying the Bayesian optimization algorithm, an initial exploration is performed where the interesting areas of optimization for the tessellation edge size are sought. This initial exploration is performed by simply comparing the results for different edge sizes.

8. Results

As a result of this research a reciprocal frame designer tool is developed, that can be used as the black-box function for the parametric optimization. The reciprocal frame designer allows the user to design and optimize reciprocal frames for certain dimensions based on 5 parameters; the tessellation pattern, tessellation edge size, tessellation density gradient, scale factor, and eccentricity. Figure 22 shows reciprocal frames for the different tessellation patterns that are generatively designed by the reciprocal frame designer.

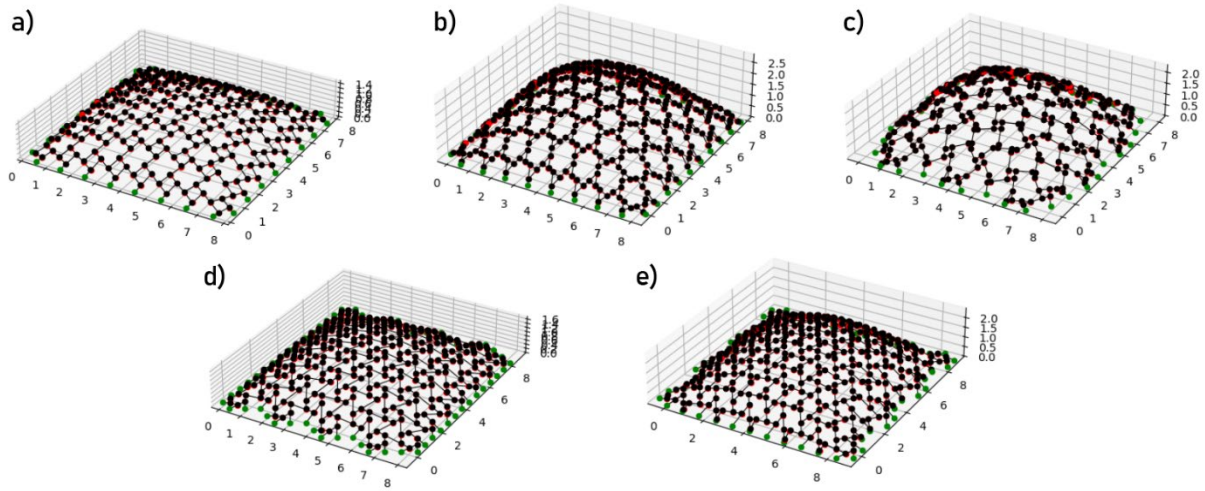

Figure 22: Reciprocal frame geometry generated by the reciprocal frame designer for different tessellation patterns: a) square, b) triangle, c) snub-square, d) hexagon and e) trihexagon

The reciprocal frame designer optimizes the cross sections to have a unity check as close as possible to the maximum unity check based on the load conditions that are provided by the user. The results of the cross section optimization for different sheet thicknesses are visualized in Figure 23. As can be seen in the figure, each beam has a variable height where the heights are generally thicker mid-span.

In Figure 23, it can also be seen that when the beam thickness become too large, each element is limited to the minimum beam height. Hence, there is almost no difference between the section heights for 30mm and 40mm thick beam elements.

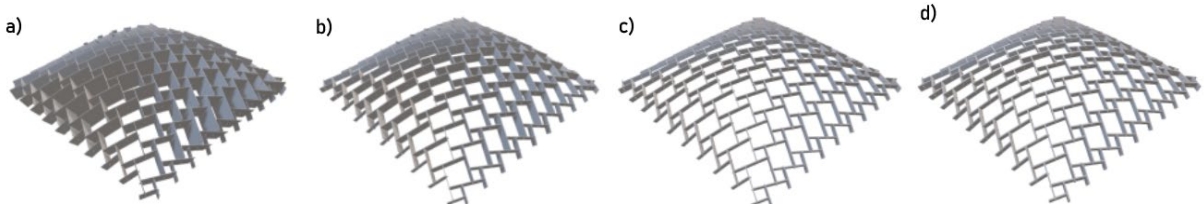

Figure 23: Cross-section optimized reciprocal frame for an 8x8m square tessellation with an edge size of 1m where the sheet thickness is; a) 15mm, b) 21mm, c) 30mm and d) 40mm

Parametric optimization results

The results of the parametric optimization are based on a specific case study where an 8x8m reciprocal frame is designed on a 3m heigh roof. The wind loads are determined according to Dutch wind area II (unbuilt) and the maximum unity checks are 0.8. The structure is of consequence class II and the density of the cladding is assumed to be 0.2 kN/m^2. It is assumed that the structural elements should be retrieved from 2440x1220mm plywood sheets.

The results of the initial exploration for the square tessellation (with a center height of 1m) are visualized in Figure 24. In the graph, it is clearly visible that there is a local minimum in the number of sheets when the edge size is low enough to fit two rows of elements on the plywood sheets. Furthermore, there is an upward trend before the dip because the height of the elements increases when the elements are longer. This is caused by the fact that there is an increased moment in the individual beam members, and the buckling length is increased. This graph would be steeper when looking at the volume of the beams, but because the element lengths are unfavorable in terms of retrievability from the plywood sheets, there is more material loss for tessellation edge sizes that are slightly larger than the local minimum.

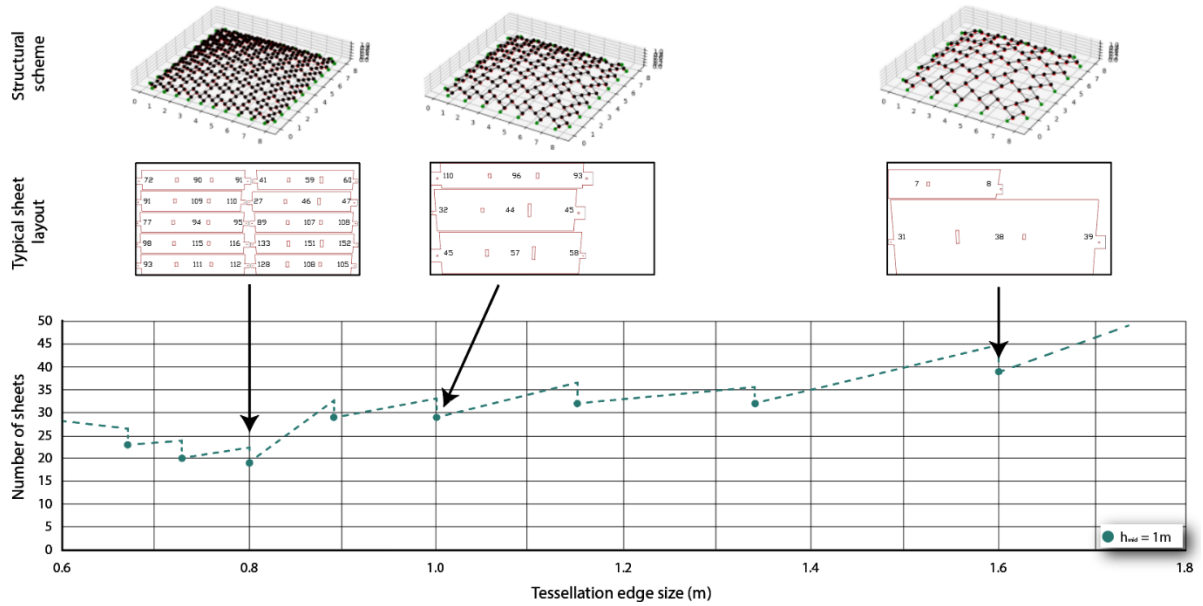

Figure 24: Initial exploration for Square tessellation pattern with center height h_{mid} = 1m

When the initial exploration is performed for other center heights, generally the results are quite similar (see Figure 25). However, when the center height is increased, the local minimum slightly moves towards smaller tessellation edge sizes. This is caused by the fact that the beam elements are stretched to be able to obtain a larger curvature with the same amount of elements.

Additionally, a more optimal result is obtained when the center height is 0. This is only the case for this tessellation pattern. For other patterns, the amount of sheets increases when the tessellation edge size increases. This difference is caused by the fact that the stress concentrations are lower when the holes

in the beam are not rotated (so when the beams are perpendicular). Additionally, the square pattern is efficient when flat because the joining elements are loaded purely in bending due to the fact the beam are perpendicular. This means that there is little normal force in the structure, meaning that no buckling behaviour prevents the elements to be long.

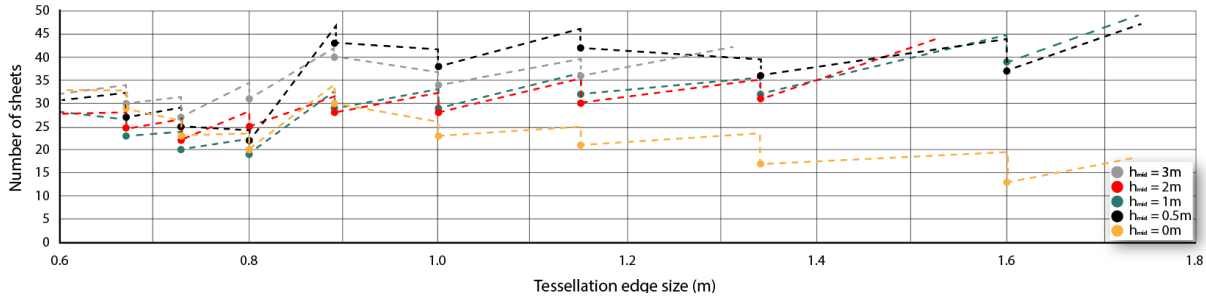

Figure 25: Full initial exploration for Square tessellation pattern

Since this behaviour is not seen in the other tessellation patterns, and this research is focused on three dimensional reciprocal frame. These low results are omitted from further parametric optimization.

For the other tessellation patterns, a similar initial exploration has been performed, resulting in the following areas of interest for the tessellation edge sizes:

- Square tessellation pattern: 0.73 – 0.8m
- Triangle tessellation pattern: 0.83 – 1.03m
- Snub-square tessellation pattern: 0.74 – 1.0m
- Honeycomb tessellation pattern: 0.43 – 0.5m
- Trihexagon tessellation pattern: 0.55 – 0.74m

The areas of interest focus on significantly smaller edge sizes for the tessellations including hexagons (honeycomb and trihexagon). This is caused by the fact that an equilateral hexagon is significantly larger than for instance an equilateral square.

When the area of interest is known, the final parametric optimization can be performed using the Bayesian optimization algorithm. To be able to see the direct influence of the sheet thickness on the amount of material that is used, the Bayesian optimization algorithm is applied for an edge size of: 15mm, 21mm, 30mm and 40mm. The results of the Bayesian optimization are summarized in Figure 26. When a beam is loaded in pure uniaxial bending – and influences like lateral torsional buckling are neglected – the beam gets more efficient when the height becomes larger with respect to the width. This is not the case for reciprocal frames because the bending is biaxial. Therefore, it can be seen that when the beam thickness is too small, the volume of sheets required increases significantly. Additionally, when elements are larger, it becomes increasingly more difficult to efficiently pack the beam elements into the bins (read: sheets).

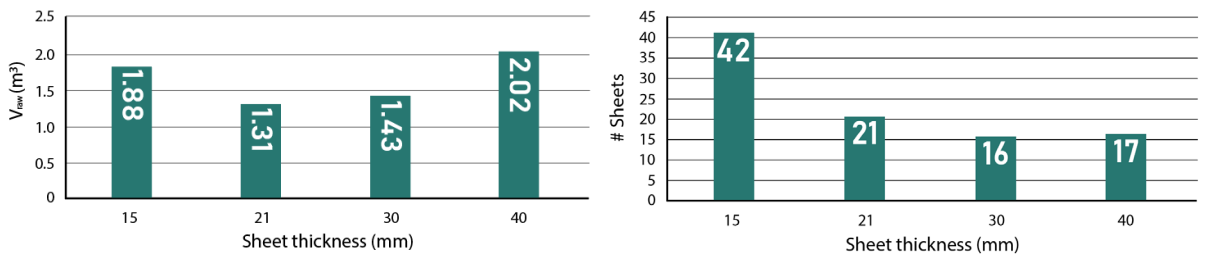

Figure 26: Results of Bayesian optimization for the square polygon tessellation. left: volume of plywood sheets required, right: number of plywood sheets required.

When expressing the result of the Bayesian optimizations in terms of amount of sheets required, it is noticeable the effect of the lower sections can be used to create a reciprocal frame with 30mm thick

elements is not significant enough to result in a lower sheet volume that is used. These results are relatively similar for each tessellation pattern, where 21mm is the most efficient sheet thickness. The only outlier that is found is the trihexagon tessellation pattern, where 30mm thick sheets are the most efficient. For the tessellation patterns with a relatively narrow search region in terms of edge size (square and triangle), the resulting optimal shape has the same edge size for all sheet thicknesses. For the other patterns, the optimal edge size is smaller for thin sheets compared to the optimal edge size for thicker sheets.

The influence of the tessellation density gradient and the scale factor are visualized in Figure 27. Generally, this behaviour is observed for each tessellation pattern. From the graph of the scale factor, it can be concluded that when the scale factor is lower, generally, the structure becomes more efficient. In a 3d reciprocal frame, this can be explained by the fact that the smaller the scale factor gets, the more the structure behaves like a normal space frame. The normal forces have to transfer a shorter path towards adjacent nodes, resulting in less out-of-plane bending.

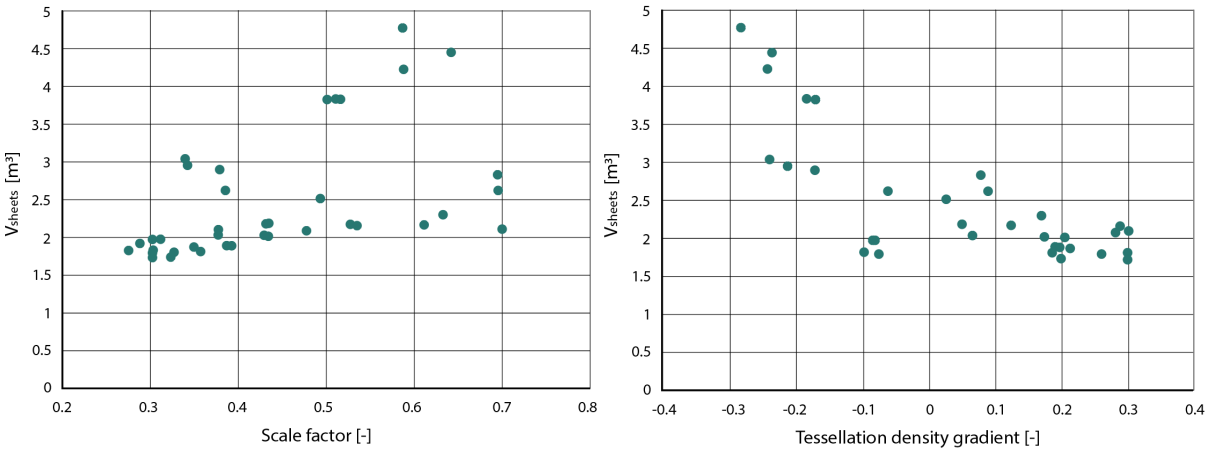

Figure 27: Scale factor (left) and tessellation density gradient (right) plotted against the volumes of sheets obtained from the Bayesian optimization of an 8x8m square tessellation reciprocal frame

The tessellation density gradient parameter is suggested in this research as it can enable a more efficient reciprocal frame by creating more density. Generally, this behaviour can be confirmed by the data that was obtained during the parametric optimization; when the tessellation density gradient is positive, the amount of sheets is reduced (see Figure 27).

In the results however, another phenomenon can also be observed. When the tessellation density gradient is slightly negative, optimal results are also found. When the reciprocal frame is translated from 2d to 3d, the beam elements are stressed as the nodes are moved in z-direction, but not in the x- or y-direction. A slightly negative tessellation density gradient counteracts this behaviour, and enables the beam elements to be more similar in length. This makes packing the elements in the available sheet size a lot more efficient.

In the optimal shape after optimization for each of the tessellation patterns is visualized. As can be seen in the figure, a high tessellation density gradient seems to have been the most efficient only for the square tessellation pattern, where the density is significantly higher in the center of the structure. However, solutions for the same tessellation pattern were found that uses the same amount of sheets. For the other tessellations the most optimal geometry has a slightly negative density gradient (between -0.05 and -0.1). This means that the optimization in that case was production focused instead of structurally focused.

Comparing tessellation patterns

Figure 29 shows a direct comparison between the tessellation patterns. The square and triangle tessellation patterns seem to be equally efficient after optimization, as the same amount of sheets are required to make those reciprocal frames.

The snub-square tessellation pattern. Is slightly less efficient. There are multiple reasons to be found for the reduced efficiency. Firstly, it is impossible to fit the tessellation exactly to the 8x8m plan. This means that an additional, unnecessary, part is added to the span of the structure. Another reason for the reduced efficiency is the fact that the beam elements do not have an equal length due to the combination of triangles and squares in the pattern.

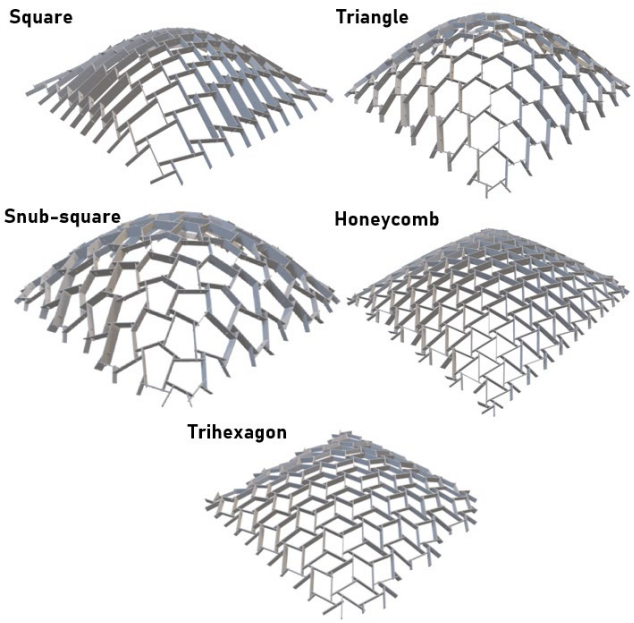

Figure 28: Most efficient reciprocal frame geometry for each tessellation pattern found by applying the Bayesian optimization algorithm

The honeycomb structure is also less efficient compared to the triangle and square pattern. The reason for this cannot necessarily be found in the structural behaviour. The difference in this case is found by looking at the number of beams required to make the tessellation. The honeycomb pattern uses significantly more elements compared to the other patterns (370 for the honeycomb tessellation versus 220 for square tessellation). The reason for this can be found by the fact that a small edge size must be used to create elements that are short enough to be packed efficiently on the sheets. Each element creates an automatic additional loss of material caused by the tenons on the ends of the beams. Additionally, similar to the snub-square pattern. It is impossible to exactly fit the polygon tessellation on the 8x8m plan. This means that some additional span is created when applying this pattern.

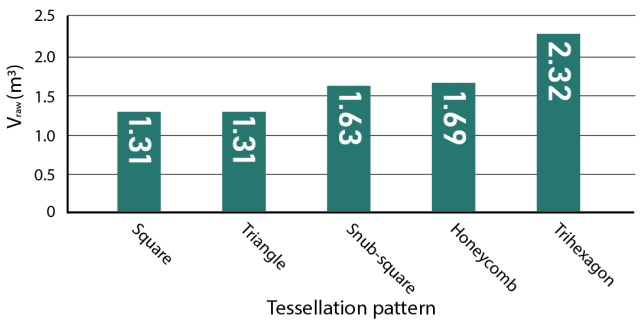

Figure 29: Comparison of sheet volume required to make an 8x8m reciprocal frame for each tessellation pattern

Finally, the trihexagon pattern seems to be significantly less efficient compared to the other tessellation patterns. Besides the reasons posed for the other tessellation patterns, this tessellation seems to be structurally significantly less efficient. A similar amount of sheets is used for the pattern when compared to the snub-square and honeycomb pattern. However, in the case of the trihexagon pattern, the sheets have a thickness of 30mm instead of 21mm.

9. Conclusion

To answer the research question, a reciprocal frame designer tool has been developed that generatively designs a plywood reciprocal frame and optimizes the cross sections of the individual cross sections in the structure. As an output, digital manufacturing data is generated that can be used to automatically fabricate the components that make up the reciprocal frame.

From the parametric optimization results, it can be concluded that the structure does not necessarily have to be optimal if only the individual cross-sections are optimized. There is a large potential for optimization by optimizing or tweaking the parameters that make up the generative design. Each of these parameters have a significant influence on the resulting amount of material (plywood sheets) required. The following conclusions can be drawn from the parametric optimization. *Note: these conclusions are based on the parametric optimization of the specific design case as described previously.*

(1) The tessellation pattern is of significant influence on the resulting amount of material required when designing a reciprocal frame out of plywood. In the example case that was used for the parametric optimization, the triangular and square tessellation are the most efficient patterns.
(2) The edge size is another significant parameter when optimizing a reciprocal frame structure. When optimizing this parameter in the initial exploration, it was observed that this parameter clearly shows the difference in optimizing for structural volume or raw material. Since the focus in this research is on optimizing for raw material, it can be seen that there is a large drop in amount of sheets required when the edge size is as such that two rows of beam elements can be fitted on a plywood sheet. The resulting optimum however does not represent the optimum when designing for the volume of the structural elements.
(3) Local minima in raw material usage are observed when the edge sizes are as such that it enables the polygon tessellation to fit the rectangular plan as closely as possible. This is the case because if the tessellation does not fit the plan closely, an additional, unnecessary, span has to be covered.
(4) The scale factor that is used in the center-to-center method also influences the resulting amount of plywood sheets that are required. For the example case, it was found that decreasing the scale factor to the lower bound generally gives more optimal solutions. The influence of this parameter is less significant than the edge size or tessellation pattern, but can be used to tweak the structure to become more optimal.
(5) The influence of the eccentricity parameter is difficult to define, as the resulting curvature of the reciprocal frame is not only a function of the eccentricity, but also the density gradient, scale factor and edge size.
(6) The influence of the curvature, however, can be found especially in the initial exploration. The center height in the structure rather significantly influences the resulting number of plywood sheets. The sweet spot of the curvature is dependent on the tessellation pattern (as well as the other parameters). The sweet spot is found by balancing between the reduction of the moment in the center of the frame and the out-of-plane bending moment and normal force in the elements.
(7) The tessellation density gradient can be used to optimize the reciprocal frames in two ways. One focusses on optimizing the structural behaviour, whilst the other focusses on optimizing for the cutting loss. When the tessellation density gradient is positive (i.e. the density is higher in the middle of the structure), there are more beam elements where the moments are higher, resulting

in a more efficient structure. When the tessellation density gradient is slightly negative, the lengths of the beam elements become more equal. This makes retrieving the elements from the plywood sheets more efficient, resulting in fewer sheets required to make the structure.

(8) Finally, the sheet thickness significantly influences the volume of the plywood sheets that are required, as well as the most optimal reciprocal frame geometry. When the sheet thickness becomes too large, elements have the minimum beam height making the structure less efficient. And when the sheet thickness becomes too low, elements become too high making it less efficient to retrieve them from the plywood sheets. For the example reciprocal frame dimensions, 21mm is the most efficient plywood sheet thickness.

To conclude, the reciprocal frame design tool can effectively be used in combination with the Bayesian optimization algorithm to find the optimal reciprocal frame for a certain rectangular floor plan under a set of boundary (load) conditions. This research proposes an approach for designing and optimizing reciprocal frames in which multiple assumptions were made. These assumptions were made to find the structure with the lowest material required, however it cannot be guaranteed that these assumptions led to the most optimal end result.

10. Recommendations

The proposed approach for optimally designing reciprocal frames from plywood structures is not guaranteed to be the most efficient method. Therefore, in future research it might be useful to propose other design methods or tweak the method proposed in this research with different initial design parameters/choices. For instance the element shape was determined by comparing four proposed beam designs. There might however be other designs that prove to be more efficient. Further research on the optimal beam morphology could result in more efficient plywood reciprocal frames.

Additionally, the approach of finding the reciprocal frame geometry is based on multiple assumptions. Firstly, in this research the method of transforming the tessellation to a reciprocal frame is the center-to-center method. This method was applied because it enables a quick and straightforward determination of reciprocal frame geometry. However, the resulting structure might structurally not be the most efficient.

The results of the parametric optimization in this research are limited to one example case of an 8x8m reciprocal frame with a specific set of location parameters and for 2.4x1.2m sheets. The effect and influence of the design parameters is not expected to behave significantly different when applied to other dimensions or locations. However, for the quality of the results, it is advised to apply the parametric optimization to multiple designs to check the consistency of the influence of the parameters and the results.

Finally, the resulting structures have not been produced in true scale. Therefore, it is advisable to test the structure in a true scale scenario to see if the expected structural and connection behaviour occurs in real life.

References

[1] Dutch Green Building Council, “Whole life carbon: position paper,” Den Haag, Sep. 2021. Accessed: Nov. 03, 2022. [Online]. Available: https://www.dgbc.nl/publicaties/position-paper-whole-life-carbon-44

[2] “PE LCA study of US sawn hardwood,” 2012. Accessed: Jan. 22, 2024. [Online]. Available: https://www.americanhardwood.org/fileadmin/docs/

[3] Q. Nguyen, “How Sustainable Is Plywood? Here Are the Facts.” Accessed: Apr. 22, 2023. [Online]. Available: https://impactful.ninja/how-sustainable-is-plywood/

[4] S. R. Kellert, J. Heerwagen, and M. Mador, *Biophilic Design: The Theory, Science and Practice of Bringing Buildings to Life*. John Wiley & Sons, 2008.

[5] T. Godthelp *et al.*, “The Timber Reciprocal Frame Designer: Free Form Design to Production,” 2019. [Online]. Available: https://www.researchgate.net/publication/336642227

[6] D. Parigi, M. Sassone, and P. Henning Kirkegaard, "Hybrid optimization in the design of reciprocal structures," 2014. [Online]. Available: https://www.researchgate.net/publication/264890660

[7] Y. Su, M. Ohsaki, Y. Wu, and J. Zhang, "A numerical method for form finding and shape optimization of reciprocal structures," *Eng Struct*, vol. 198, Nov. 2019, doi: 10.1016/j.engstruct.2019.109510.

[8] Y. Anastas, L. Rhode-Barbarigos, and S. Adriaenssens, "Design-to-construction workflow for cell-based pattern reciprocal free-form structures," *Journal of the International Association for Shell and Spatial Structures*, vol. 57, no. 2, pp. 159–176, Jun. 2016, doi: 10.20898/j.iass.2016.188.737.

[9] A. Habraken and T. Godthelp SIDstudio bv, "Digital path towards Timber Reciprocal Frame Structures," 2021.

[10] J. Rizzuto, M. Saïdani, and J. C. Chilton, "Polyhedric space structures using reciprocally supported elements of various cross-sections," *Journal of the International Association for Shell and Spatial Structures*, vol. 42, pp. 149–159, 2001.

[11] O. Popovic Larsen, "RECIPROCAL FRAME ARCHITECTURE," 2008. Accessed: May 11, 2023. [Online]. Available: https://casaeco.files.wordpress.com/2012/03/reciprocal-frame-architecture.pdf

[12] N. Mellado, P. Song, X. Yan, C.-W. Fu, and N. J. Mitra, "Computational Design and Construction of Notch-Free Reciprocal Frame Structures," pp. 181–197, 2014, doi: 10.1007/978-3-319-11418-7_12ï.

[13] P. Song, C.-W. Fu, P. Goswami, and J. Zheng, "Reciprocal Frame Structures Made Easy."

[14] Y. Su, M. Ohsaki, Y. Wu, and J. Zhang, "A numerical method for form finding and shape optimization of reciprocal structures," *Eng Struct*, vol. 198, Nov. 2019, doi: 10.1016/j.engstruct.2019.109510.

[15] J. Schlick, "Is Water Jet Cutting Wood Possible?" Accessed: Jun. 04, 2023. [Online]. Available: https://www.techniwaterjet.com/can-waterjet-cut-wood/

[16] "CNC-Cut-to-Size-Guidelines," Darra, 2020. Accessed: Jun. 04, 2023. [Online]. Available: https://www.plywoodandpanel.com.au/wp-content/uploads/2020/03/CNC-Cut-to-Size-Guidelines.pdf

[17] W. D. Pilkey, D. F. Pilkey, and Z. Bi, *Peterson's Stress Concentration Factors*, 4th ed. Hoboken: John Wiley & Sons, 2020. doi: 10.1002/9781119532552.

[18] Dr. John McGuire, "Notes on Semi-Rigid Connections," Jul. 1995. Accessed: Nov. 03, 2023. [Online]. Available: https://femci.gsfc.nasa.gov/semirigid/

[19] E. Wieringa, A. S. J. Suiker, A. P. H. W. Habraken, and G. J. Rozemeijer, "Finite Element Analysis of Interlocking Timber Connections in Plywood Diaphragm Floors: Optimizing Form for Strength," 2023. Accessed: Nov. 03, 2023. [Online]. Available: https://pure.tue.nl/ws/portalfiles/portal/306714154/Wielinga_1017980_ABP_Suiker_MSc_thesis.pdf

[20] T. Wang, Y. Wang, R. Crocetti, and M. Wålinder, "In-plane mechanical properties of birch plywood," *Constr Build Mater*, vol. 340, Jul. 2022, doi: 10.1016/j.conbuildmat.2022.127852.

[21] K. Tejlgaard and B. Jepsen, "Dome of Visions," Behance. Accessed: Mar. 28, 2024. [Online]. Available: https://www.behance.net/gallery/8369477/Dome-of-Visions

[22] I. A. P. H. W. Habraken and I. G. J. Rozemeijer, "Finite Element Analysis of Interlocking Timber Connections in Plywood Diaphragm Floors: Optimizing Form for Strength," 2023.

[23] A. N. Zehmakan, "Bin Packing Problem: A Linear Constant-Space 3/2-Approximation Algorithm." Accessed: Jun. 11, 2023. [Online]. Available: https://arxiv.org/ftp/arxiv/papers/1610/1610.08820.pdf

[24] J. Jylänki, "A Thousand Ways to Pack the Bin-A Practical Approach to Two-Dimensional Rectangle Bin Packing," 2010. Accessed: Jun. 11, 2023. [Online]. Available: http://pds25.egloos.com/pds/201504/21/98/RectangleBinPack.pdf

[25] S. Albers, "Bin packing 1. Problem definition and general observations," 2008. Accessed: Jun. 11, 2023. [Online]. Available: https://ac.informatik.uni-freiburg.de/lak_teaching/ws07_08/algotheo/Slides/13_bin_packing.pdf

[26] P. I. Frazier, "A Tutorial on Bayesian Optimization," Jul. 2018, [Online]. Available: http://arxiv.org/abs/1807.02811